Gu *et al. Chem. Biol. Technol. Agric.* (2023) 10:113
https://doi.org/10.1186/s40538-023-00487-4

Chemical and Biological Technologies in Agriculture

RESEARCH

Open Access

Synergistic mechanism of *Bacillus subtilis* Czk1 combined with propiconazole and tebuconazole mixtures against *Pyrrhoderma noxium*

Zi-wei Gu[1,2†], Jian-hang Yin[2,3†], He Wu[4†], Yan-qiong Liang[2], Wei-huai Wu[2], Ying Lu[2], Rui Li[2], Shi-bei Tan[2], Chun-ping He[1,2,3*] and Ke-xian Yi[1,2,5,6,7*]

Abstract

Background Brown root rot disease is one of the devastating diseases in the rubber production process. It is not easy to be detected in the early stage of the disease. Our early research revealed that the rubber tree brown root rot fungus *Pyrrhoderma noxium* Pn006 was effectively inhibited by *Bacillus subtilis* Czk1 and 25% propiconazole–tebuconazole, and that the two agents might work in synergy. Therefore, in this investigation, we used non-targeted metabolomic method to evaluate the synergistic mechanism of *B. subtilis* Czk1 and 25% propiconazole–tebuconazole on *Pyrrhoderma noxium* Pn006.

Results Metabolomics analysis identified 708 unique metabolic markers, including mainly lipids and lipid-like molecules, organic acids, alcohols, ketones, alkaloids and their derivatives, nucleotides and their analogues, benzene ring compounds and amino acids and their derivatives. Further screening identified 105 key metabolic markers that could be potential biomarkers to reveal the mechanism of biocontrol bacteria and chemical fungicides combination synergy. Three key metabolic pathways were found in pathway enrichment, including linolenic acid metabolism, benzoic acid degradation, and valine, leucine and isoleucine degradation.

Conclusions The mechanism might be related to the influence of the energy supply and cell functional integrity of pathogenic fungal cells.

Critical relevance statement A metabolomic method was utilized to investigate the synergistic effects of *B. subtilis* Czk1 and 25% propiconazole–tebuconazole use on *Pyrrhoderma noxium* Pn006.

Key points

1. Optimal combination ratio of *B. subtilis* Czk1 and 25% propiconazole–tebuconazole and its mechanism of action.
2. Mechanism of potentiation of *B. subtilis* Czk1 and 25% propiconazole–tebuconazole associations identified by metabolites.

†Zi-wei Gu, Jian-hang Yin and He Wu contributed equally and should be considered as co-first authors.

*Correspondence:
Chun-ping He
hechunppp@163.com
Ke-xian Yi
yikexian@126.com
Full list of author information is available at the end of the article

3. Provides a reference for pesticide reduction and efficiency technologies.

Keywords Rubber tree root rot disease, *Bacillus subtilis* Czk1, 25% propiconazole–tebuconazole, *Pyrrhoderma noxium*, Cell metabolomics

Graphical Abstract

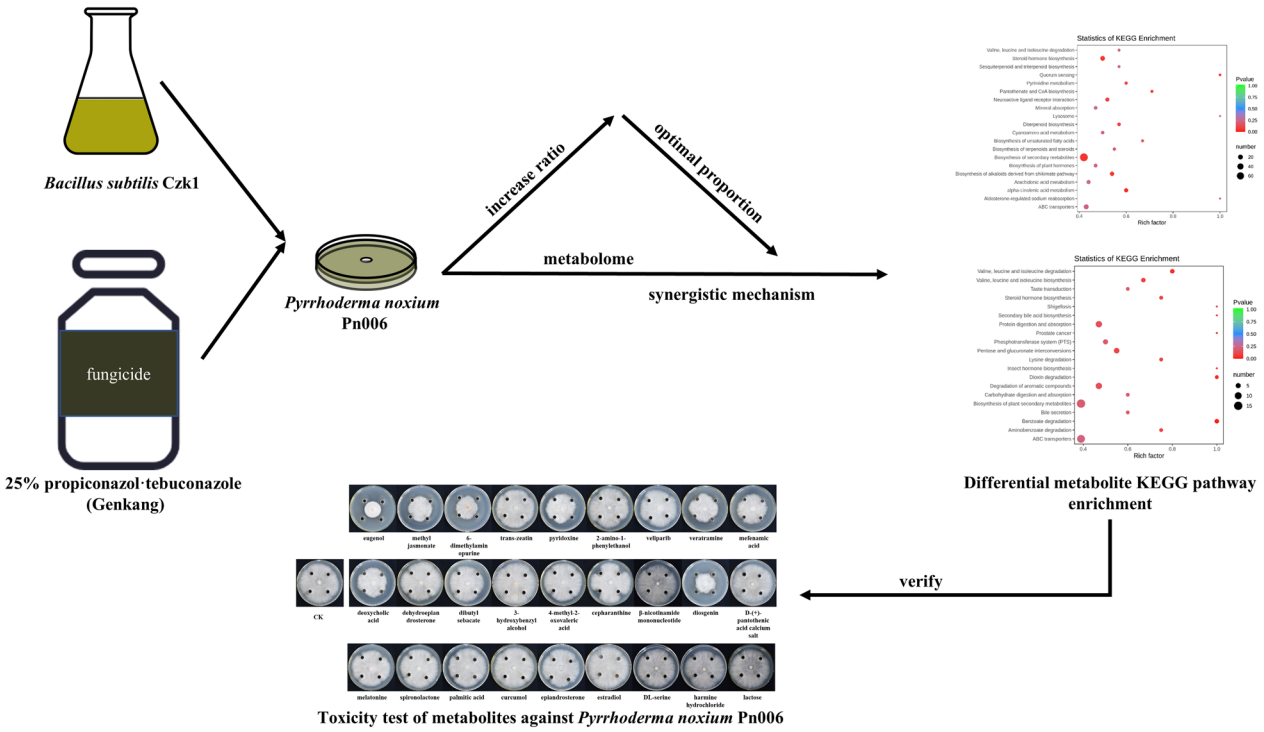

Introduction

Root rot disease is a serious kind of disease on rubber trees, commonly occurring in rubber plantation areas around the world, and can be caused by a variety of fungal infections [1]. The disease is spread mainly through root contact, causing root rot and wilting of plants [2]. There are seven types of root rot diseases found in China: red root rot disease, brown root rot disease, white root rot disease, purple root rot disease, black root rot disease, stink root rot disease and ustulina root rot disease. Among them, *Pyrrhoderma noxium* (Corner) L.W. Zhou & Y.C. Dai (former name: *Phellinus noxius* (Corner) G.H. Cunn. [3]) is second only to red root rot disease in China, with an incidence of more than 2%, and more than 10% in severe forest segments [4]. However, its lethality rate is much higher than that of other root rot diseases in China, which is one of the devastating diseases in the rubber production process [5]. More than 200 different host plant species are at risk from *Pyrrhoderma noxium*, which can remain in the soil for more than 10 years and spread when healthy plant tree roots come contact touch with the pathogen or germ-carrying leftovers [2, 6]. One of the pests in Chinese quarantine is *Pyrrhoderma noxium* [3]. The most effective control method for this disease is still chemical control. Brown root rot disease has the characteristics of fast spreading and stealthy, so it is not easy to detect in the early stage of the disease. In addition, although chemical control is direct and effective, long term and single use is easy to cause a decline in the effectiveness of prevention and soil ecological insecurity in rubber forests [7, 8].

25% propiconazole–tebuconazole (Genkang) is a triazole fungicides. Triazole fungicides are broad-spectrum fungicides that are widely used to control diseases caused by ascomycetes, deuteromycotina and basidiomycetes [9]. By interacting with the C-14-α-demethylase of cytochrome P450 of pathogenic fungi, the biosynthesis of ergosterol of fungi is inhibited and the integrity of cell membranes is damaged to control the disease [10].

Tebuconazole is one of the most widely sold pesticides in the world, and widely used for controlling many plant fungus diseases [11]. Propiconazole is used to restrain the fungal growth on vegetables, fruits and cereals and it is widely used in crop fields as a foliar spray [12]. But if a single chemical fungicide is used repeatedly, harmful fungus will develop a resistance to it [13]. The approach of using bio-chemical synergistic control of plant diseases can enable the complementary benefits of biological and chemical control, which can reduce the application of chemical pesticides [14, 15], but also slow down the development of pathogen resistance and environmental pollution [16], and promote the colonization of biological control bacteria and stability of biocontrol effect [17, 18], and may also produce synergistic effect [19, 20]. In particular, with the ongoing research on synergistic biological and chemical control, many bacterial biocontrol agents have been developed and identified as safer and more sustainable control measures than synthetic pesticides [21, 22]. In recent years, in the fight against soil-borne plant diseases, many positive results have been seen [23, 24].

Bacillus is a biotrophic bacterium that plays an important role in the control of plant pathogens. They can not only protect plants from pathogens but also promote plant growth through repopulation, secretion of compounds and provision of nutrients [25]. *Bacillus subtilis* is a bacterium in the genus *Bacillus*, which is widely distributed in nature, harmless to humans and animals, and has efficient and broad-spectrum antifungal activity [26]. *Bacillus subtilis* can colonize on the root surface of host plants and in host plants. It can also secrete antimicrobial substances that inhibit the growth of plant pathogens and induce systemic resistance in plants, which will prevent disease infestation [22, 27]. However, using biocontrol bacteria alone to control plant diseases, frequently has the drawbacks of poor colonization potential, unstable effects and sluggish effects. The combined application of biocontrol bacteria and chemical fungicides can not only stabilize the control effect of biocontrol bacteria but also reduce the use of chemical fungicides [28]. The combination of biocontrol agents (BACs) and chemical fungicide tebuconazole to control okra powdery mildew, and the control effect was significantly more effective than the chemical fungicide alone [29]. In addition to having potent inhibitory and controlling effects on tobacco root rot, *Bacillus velezensis* isolated from soil can also encourage the growth and root development of tobacco plants [30]. More successfully than carbendazim alone, two biologically released bacteria, *B. cepacia* c91 and *B.megaterium* c96, respectively, attenuated tomato green blight and root rot [31]. The screening of antagonistic microorganisms [32], as well as the identification and analysis of inhibitory chemicals [5, 33, 34], are the main areas of current study in rubber tree root rot disease biocontrol technology. Li et al. measured the antagonistic effects of 9 strains of *Trichoderma* on the rubber tree pathogen responsible for brown root rot and ultimately screened out 3 strains of *Trichoderma* strains with strong antagonistic effects [35]. Zahari et al. extracted the antifungal chemical from *Catharanthus roseus*, to investigate the antifungal compound of inhibitory effect on *Rigidoporus microporus*, *Ganoderma philippi*, and *Phellinus noxius*. The results showed that the extract was effective against *Ganoderma philippii* and *Rigidoporus microporus* but not effective against *Phellinus noxius* [36]. He et al. identified the lipopeptides produced by *Bacillus subtilis* Czk1. The bacterial isolate exhibits strong antagonistic activity against *Ganoderma pseudoferreum*, *Phellinus noxius*, *Helicobasidium compactum*, *Rigidoporus lignosus*, *Sphaerostilbe repens*, and *Colletotrichum gloeosporioides* [37]. There are few reports on the mechanism of the synergistic effect of bacterial and fungicide compounding [15].

The study of all small molecule compounds of quantitative, qualitative, and dynamic changes in organisms, organs, tissues, or cells throughout a certain amount of time or in a given environment is known as metabolomics. It identifies the functional characteristics and processes that take place when organisms are stimulated by examining the altering patterns of metabolic conditions in living things. It is crucial to the study of the interactions between plants and microbes, transgenic breeding, and the validation of gene function. Physiological and biochemical analyses of the mechanisms are possible [38]. Steroidal compounds and fatty acid derivatives were found to be more abundant in infected roots when comparing the metabolites of oil palm roots with and without *Ganoderma boninense* infection, indicating that these metabolites are crucial for pathogen defense [39]. It is hypothesized that metabolites like sugars, organic acids, and amino acid derivatives may be connected to the metabolic level defense response of soybean against soybean to *P. sojae* based on the changes of these DAMs in response to *P. sojae* infection in different lines and at different time points, as well as the differences in the contents of these differentially accumulated metabolites between the resistant line and the susceptible line [40]. The Epichlo endophytes strains NEA12 and NEA23 exhibit strong antifungal activity. The discovery that NEA12 and NEA23 create antifungal compounds in a symbiotic relationship was supported by metabolite analysis of the endophytes and bioactivity study of the metabolites [41]. On barley that had received a *Gibberella zeae* inoculation, a metabolic analysis was carried out. Three metabolic pathways linked to susceptibility were found,

metabolites greatly slowed down the mycelial development of *G. zeae* in vitro [42].

Although prior research has demonstrated that the combination of *Bacillus subtilis* Czk1 and a chemical fungicide known as Genkang has strong inhibition activity and synergistic effects against red root rot and brown root rot pathogens of rubber trees, studies on its mechanism of action have not been clarified [43]. Therefore, in this study, non-target metabolomics technology based on Liquid chromatography–tandem mass spectrometry (LC–MS/MS) was utilized to investigate the target and mechanism of exogenous substances, search for endogenous differential metabolite changes of Czk1 under the combined stress of 25% propiconazole–tebuconazole (Genkang), and provide new target sites for the design of new drugs molecular biosynthesis.

Materials and methods

Materials and chemicals

The biocontrol bacterium *B. subtilis* Czk1(GenBank: GQ395245.1) and the pathogen *Pyrrhoderma noxium* Pn006 (GenBank: KC255249.1) were both isolated, identified and preserved by the Tropical Food and Specialty Crop Diseases Research Group, Institute of Environment and Plant Protection, Chinese Academy of Tropical Agricultural Sciences. 25% propiconazole–tebuconazole (Genkang, microemulsion, 5% propiconazole and 20% tebuconazole) microemulsion produced by Guangdong Dafeng Plant Protection Technology Co., Ltd. The mass spectrometer (QTOF/MS-6545, Aglient, Germany), ultra-high performance liquid chromatography (1290 Infinity LC, Aglient, Germany), vortex mixer (MIX-200, Shanghai, China), automatic sample rapid grinder (Tissuelyser-64, Shanghai, China) and acetonitrile (chromatographic purity) were purchased from Aglient Technologies, Shanghai Jingxin Industrial Development Co., and Eppendorf AG, Germany, respectively.

Strain (cell) cultivation

The single colony of Czk1 was cultured in LB liquid medium (LB) and activated at 37 ℃ and 180 r/min for 12 h to obtain a seed solution. The seed solution was cultured in a fresh LB at the inoculation ratio of 5%, shaken, and fermented at 28 ℃ and 180 r/min for 72 h, and the fermentation solution was centrifuged at 4 ℃ and 12,000 r/min for 15 min. The supernatant was sterilized by a filter with a 0.22 μm pore size to obtain a sterile culture filtrate, which was stored at 4 ℃ for later use Pn006 was cultured on PDA medium (PDA) at 28 ℃ for 3 d, and Pn006 mycelium block was prepared with a hole punch with a diameter of 5 mm.

Inhibitory effect of different concentrations of Czk1 on Pn006

The culture filtrate was added to the PDA at different concentrations to make the final concentrations 10, 20, 40, 60, and 80 μL/mL, respectively. Then Pn006 was incubated in PDA dishes containing each concentration of culture filtrate, and the same amounts of LB were used as the control for constant temperature oscillation culture at 28 ℃. When the radius of the control mycelium reached 2/3 of the culture dish radius, the colony diameter was observed and recorded. ANOVA and regression analysis were performed using SPSS, and the EC_{50} of Czk1 culture filtrate to Pn006 was calculated.

Inhibitory effect of Genkang combined with Czk1 on Pn006

The effective inhibitory medium concentration solution was made using the EC_{50} value of 0.0522 g/mL for Genkang determined by Xie [43] and the EC_{50} value of Czk1 culture filtrate determined. Then the culture filtrate of Czk1 without concentration was combined with different concentrations of Genkang drug solution. The compounding agents with the volume ratio V (Czk1 culture filtrate): V (Genkang) of 0:10 (T1), 1:9 (T2), 2:8 (T3), 3:7 (T4), 4:6 (T5), 5:5 (T6), 6:4 (T7), 7:3 (T8), 8:2 (T9), 9:1 (T10) and 10:0 (T11) was prepared. Depending on the compounding agents' inhibitory rates, calculating combined virulence and evaluating the synergistic effects. The increase ratio (IR) was assessed using the Horsfall method [44], where $IR < 1$ indicates antagonism, $IR = 1$ indicates an additive effect, and $IR > 1$ indicates a synergistic effect.

Effect of Genkang combined with Czk1 on metabolites of Pn006

Sample preparation. The Czk1 culture filtrate was mixed with Genkang and added to PDA to make its concentration the same as screened for their highest synergistic ratio combination. In a petri dish containing the compound and the two single agents, a layer of cellophane was placed flat, and a Pn006 mycelial block was placed in the center of the cellophane. The control was a solution made up of an equal mixture of LB and sterile water. When the mycelium grows all over the petri dish, collect the mycelium sample, wash and absorb the water, then use liquid nitrogen to freeze for 15 min. They were separated into four groups: the compound treatment group (CG group), the Czk1 culture filtrate single agent treatment group (C group), the Genkang single agent treatment group (G group), and the blank control group (CK group), and stored at − 80 °C.

Sample pretreatment. A sample of 50 ± 2 mg was weighed into a 2 mL centrifuge tube and 500 μL of 70% methanolic water (containing 1 μg/mL of 2-chlorophenylalanine) pre-chilled at −20 °C was added. Homogenate the mixture at 30 Hz for 2 min. After homogenization, shake the mixture for 5 min and incubate it on ice for 15 min. Centrifuge the mixture at 12,000 rpm at 4 ℃ for 10 min and suck supernatant 400 μL into another centrifuge tube. Add 500 μL of ethyl acetate/methanol (V, 1:3) into the original centrifuge tube, oscillate the mixture for 5 min, and incubate it on ice for 15 min. Then centrifuge it at 12,000 rpm at 4 ℃ for 10 min and take 400 μL of supernatant. Merge the two supernatants and concentrate them. Then add 100 μL of 70% methanol water into the dried product and perform transonic treatment for 3 min. Finally centrifuge it at 12,000 rpm at 4 ℃ for 3 min, and suck 60 μL of supernatant for LC–MS/MS analysis.

Chromatography–mass spectrometry acquisition conditions. All samples were acquired by the LC–MS/MS system following machine orders. The analytical conditions were as follows, UPLC: column, Waters ACQUITY UPLC HSS T3 C18 (1.8 μm, 2.1 mm*100 mm); column temperature, 40 ℃; flow rate, 0.4 mL/min; injection volume, 2 μL; solvent system, water (0.1% formic acid): acetonitrile (0.1% formic acid); gradient program, 95:5 V/V at 0 min, 10:90 V/V at 11.0 min, 10:90 V/V at 12.0 min, 95:5 V/V at 12.1 min, 95:5 V/V at 14.0 min.

Data processing and analysis

The original data file obtained by LC–MS/MS analysis is firstly converted into mzML format by Proteo Wizard software. Peak extraction, alignment, and retention time correction are performed by the XCMS program. The "SVR" method was used to correct the peak area. Filter the peaks with a deletion rate > 50% in each group of samples. After that, metabolic identification information was obtained by searching the laboratory self-built database and integrating the public database and MetDNA. Finally, statistical analysis was carried out by the R program. Statistical analysis includes univariate analysis and multivariate analysis. Univariate statistical analysis includes Student's t-test and variance multiple analysis. Multivariate statistical analysis includes principal component analysis (PCA), partial least squares discriminant analysis (PLS-DA), and orthogonal partial least squares discriminant analysis (OPLS-DA).

Effects of metabolites on pathogenic fungus

Based on the results of the metabolome data, 27 key differential metabolites were selected to test their effects on pathogenic fungus in vitro. The 27 differential metabolites are shown in Table 1.

Table 1 Differential metabolites for testing

Serial number	CAS	Compound
1	97-53-0	Eugenol
2	1211-29-6	Methyl jasmonate
3	4871-97-0	Curcumol
4	65-23-6	Pridoxine
5	938-55-6	6-Dimethylaminopurine
6	343-27-1	Harmine hydrochloride
7	63-42-3	Lactose
8	302-84-1	DL-serine
9	1094-61-7	β-Nicotinamide mononucleotide
10	1957-10-03	Palmitic acid
11	73-31-4	Melatonine
12	54-43-0	Dehydroepiandrosterone
13	109-43-3	Dibutyl sebacate
14	57-91-0	Estradiol
15	620-24-6	3-Hydroxybenzyl alcohol
16	7568-93-6	2-Amino-1-phenylethanol
17	481-29-8	Epiandrosterone
18	1952-01-07	Spironolactone
19	83-44-3	Deoxycholic acid
20	137-08-6	D-(+)-pantothenic acid calcium salt
21	816-66-0	4-Methyl-2-oxovaleric acid
22	481-49-2	Cepharanthine
23	912444-00-9	Veliparib
24	60-70-8	Veratramine
25	61-68-7	Mefenamic acid
26	1637-39-4	Trans-zeatin
27	512-04-9	Diosgenin

Inhibitory effect of 27 key metabolites on Pn006. The 27 compounds were prepared as 5 mg/mL solutions. Using the Oxford Cup method, four Oxford Cups were placed at an intermediate distance from each PDA plate, 100 μL of the solution was added to each Oxford Cup separately, and a Pn006 mycelium block was accessed in the center of the PDA plate. Three replicates of each treatment and incubated at a constant temperature at 28 °C for 72 h. The test results were observed and noted.

Indoor toxicity determination of active metabolites on Pn006. To further understand the effect of the differential metabolites on the pathogenic fungus, the mycelial growth rate method was used. The three differential metabolites with better inhibitory effect on Pn006 were configured into different concentration gradients and added to the PDA to make drug-containing PDA plates. Six replicates of each treatment and incubated at 28 ℃ for 72 h. The concentration gradients of the three different metabolites are shown in Table 2.

Table 2 Concentration gradients of the test differential metabolites

Metabolites	Concentration gradient (μg/mL)				
Eugenol	10	20	40	80	160
Methyl jasmonate	15	30	60	120	240
6-Dimethylaminopurine	8	16	32	64	128

Results

Effect of Czk1 on the antagonistic activity of Pn006

The effects of different concentrations of Czk1 culture filtrate on the antifungal activity of Pn006 are shown in Table 3. The Czk1 has good antifungal activity against Pn006. With the increase in the concentration of Czk1 filtrate, the antifungal activity of Czk1 was enhanced gradually. When the concentration of Czk1 culture filtrate was 80 μL/mL, the inhibitory rate was 79.54% (Table 3). By employing the logarithm of the concentration as the horizontal coordinate and the odds value of the inhibition rate as the vertical coordinate in a regression analysis carried out with SPSS software, the regression equation for the inhibition of Pn006 by Czk1 was derived: $y = 0.019x + 4.308$. The EC_{50} of Czk1 against Pn006 was determined to be 36.42 μL/mL using the regression equation.

Effect of Czk1 combined with Genkang on the antagonistic activity of Pn006

The effect of Czk1 combined with Genkang on the antagonistic activity of Pn006 is shown in Table 4. When different volume ratios of V_{Czk1} culture filtrate combined with $V_{Genkang}$ were 1:9 (T2), 2:8 (T3), 3:7 (T4), 4:6 (T5), 5:5 (T6), 6:4 (T7), 7:3 (T8), 8:2 (T9), 9:1 (T10), the toxicity ratio IR was all greater than 1. The results showed that all of the above nine ratios of mycobacterial drug combinations had synergistic inhibitory effects on Pn006. The strongest synergistic effect was observed with the T3 combination (V_{Czk1}: $V_{Genkang}$ = 2:8), with a toxicity ratio of 1.49. Therefore, the T3 combination was used as the dosing concentration for the metabolomics study.

Table 3 Effect of different concentrations of Czk1 on the antibacterial activity of Pn006

Concentration (μL/mL)	Colony diameter (%)	Control effect (%)	Virulence regression equation	EC_{50} (μL/mL)
10	4.79	28.62 ± 2.09 e	$y = 0.019x + 4.308$	36.42
20	4.05	40.93 ± 0.79 d		
40	3.36	52.41 ± 1.40 c		
60	2.45	67.55 ± 0.74 b		
80	1.73	79.54 ± 0.90 a		
CK	6.51	–		

Lowercase letters indicate a statistical significance level of 0.05, with significant differences between levels not connected using the same lowercase letter and highly significant differences between levels not connected using the same uppercase letter after the same column of data

Table 4 Toxicity ratios of different combinations of Czk1 and Genkang against Pn006

V_{Czk1}:$V_{Genkang}$	Colony diameter (cm)	Observed effect (Eab) (%)	Thioritical effect (Eth) (%)	Inhibitory ratio
T1	4.02	45.37	45.37	1.00
T2	2.75	65.65	45.86	1.43
T3	2.55	68.85	46.36	1.49
T4	2.88	63.58	46.85	1.36
T5	2.74	65.81	47.35	1.39
T6	2.58	68.37	47.84	1.43
T7	2.83	64.38	48.34	1.33
T8	2.80	64.86	48.83	1.33
T9	2.78	65.18	49.33	1.32
T10	3.22	58.15	49.82	1.17
T11	3.71	50.32	50.32	1.00
CK	6.86	–	–	–

Effect of Genkang combined with Czk1 on Pn006 metabolites

Principal component analysis. Before performing difference analysis, principal component analysis (PCA) was first performed on the grouped samples for difference comparison, and the degrees of variation among the grouped samples and the samples within the group were observed. PCA model showed that in the positive and negative electron spray ionization (ESI+ and ESI−) (Additional file 1: Fig S1), there was a significant segregation trend between the blank control and compound groups (CK-CG), indicating that there was a difference in the overall metabolism of these groups. The OPLS-DA model was established by combining orthogonal signal correction and partial least squares discriminant analysis (Fig. 1). The OPLS-DA model showed that CK-CG groups were completely separated, which indicated that there were significant differences in metabolic characteristics between CK-CG groups. In both ESI+ and ESI−, the prediction parameters Q^2 of the OPLS-DA model are 0.982, which indicates that the OPLS-DA model is excellent and reliable.

Screening and identification of differential metabolites. Based on the OPLS-DA results, the metabolites that differed between groups could be initially screened from the obtained Variable Importance in Projection (VIP) of the multivariate analysis OPLS-DA model, and the screening criterion was set as VIP ≥ 1. Further screening for differential metabolites was combined with a *t*-test of $P < 0.05$ for univariate analysis and FC ≥ 2 or FC ≤ 0.5 for Fold Change (FC) values of differences. The volcano diagram (Fig. 2) shows the degree of variability of metabolites in positive and negative ion modes. A total of 2519 differential metabolites were screened, including 2109 in the positive ion mode and 410 in the negative ion mode (Table 5). Figure 2 shows the relationship between the different metabolites in each group as a Venn diagram. Through comparative analysis, positive ion mode metabolites from the CK-CG group total 594, with the majority of them being lipids and lipid-like molecules such as organic acids, alcohols, ketones, alkaloids and their derivatives, nucleotides and their analogues, benzene ring compounds, amino acids and their derivatives; In the negative ion mode, there are 114 different metabolites, most of which are lipids and lipid-like compounds, organic acids, sugars, amino acids and their derivatives, nucleotide analogues, and alkaloids. Further screening of 708 differential metabolites in the CG-CK group revealed 105 identified as key metabolites (Additional file 2: Table S1 and Table 6), which may be potential biomarkers to reveal the synergistic effect of Czk1 combination with Genkang.

Metabolic pathway analysis. Based on the results of differential metabolites, metabolic pathway enrichment was performed using KEGG (Kyoto Encyclopedia of Genes and Genomes) (Fig. 3). In positive ion mode, the significantly differential metabolic pathway enriched in the CG-CK group (Fig. 3a) was linolenic acid metabolism. In the negative ion mode, the CG-CK group (Fig. 3b) was enriched for benzoic acid degradation, dioxin degradation, and valine, leucine and isoleucine degradation. After the screening, the metabolic pathways unique to

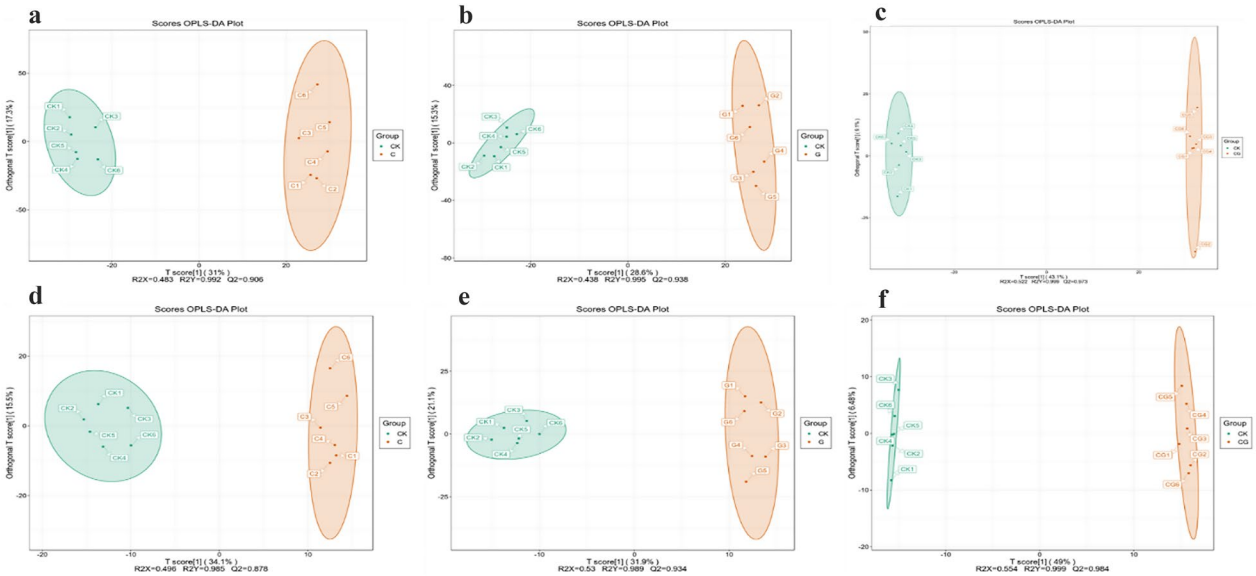

Fig. 1 Outline of the grouped OPLS-DA model. **a–c** OPLS-DA model in positive ion mode; **d–f** OPLS-DA model in negative ion mode

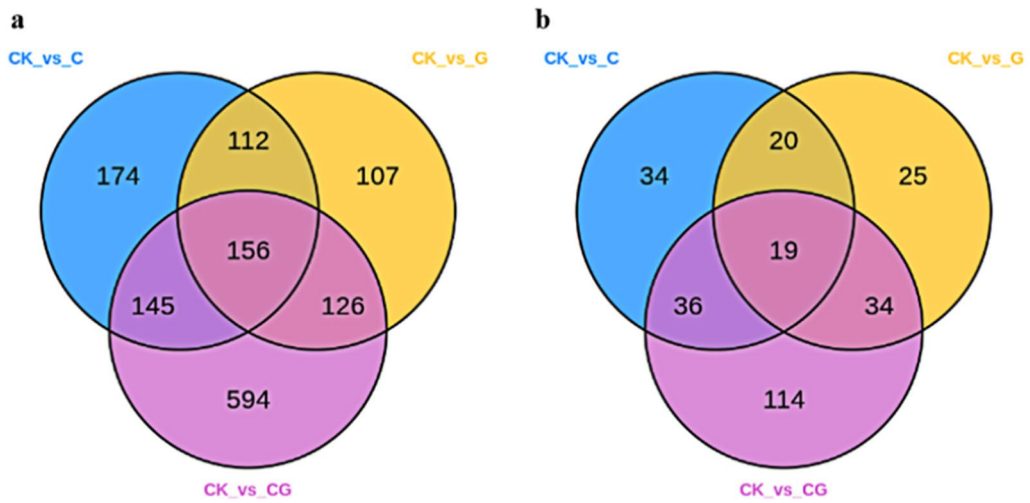

Fig. 2 Differential metabolite Wein diagram. **a** positive ion mode; **b** negative ion mode

Table 5 Number of differential metabolites in ESI+ and ESI−

Mode	Group	Metabolite	Down	Up
ESI+	CK-C	587	259	328
	CK-G	501	165	336
	CK-CG	1021	420	601
ESI−	CK-C	109	44	65
	CK-G	98	24	74
	CK-CG	203	72	131

the compound were the linolenic acid metabolic pathway, valine, leucine and isoleucine degradation pathways, and benzoic acid degradation pathway (Table 6).

In vitro inhibition of Pn006 by differential metabolites

Oxford Cup method primary screening. The differences in inhibitory effects that the 27 distinct metabolites had on Pn006, with eugenol, methyl jasmonate, and 6-dimethylaminopurine displaying the strong inhibitory

Table 6 Unique differences in metabolic pathways information of the compounding agent

Pathway	ko_ID	Unique compound	Compound	Rich factor	*P*-value
Alpha-Linolenic acid metabolism	ko00592	12	20	0.6	0.028365
Valine, leucine and isoleucine degradation	ko00280	4	5	0.8	0.038597
Benzoate degradation	ko00362	4	4	1	0.010281

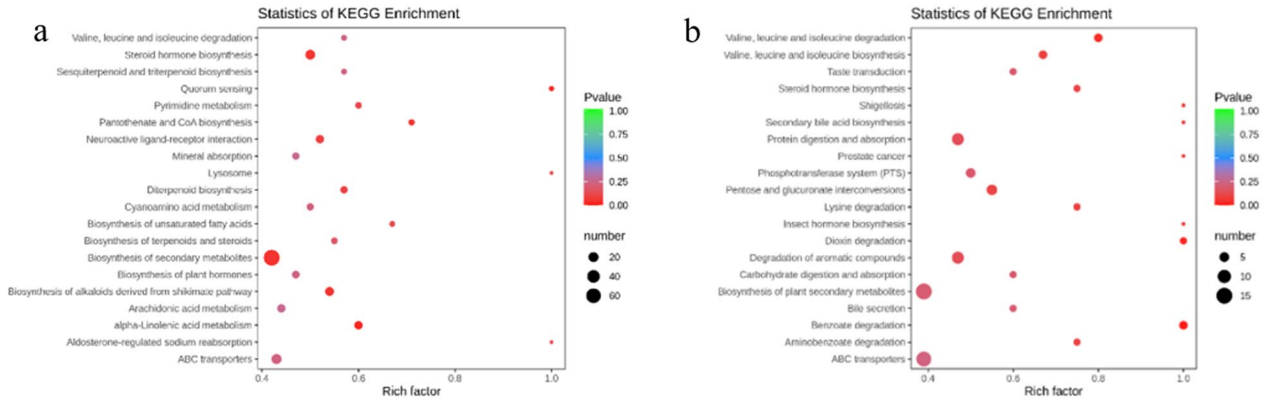

Fig. 3 Differential metabolite KEGG pathway enrichment. **a** ESI+; **b**: ESI−

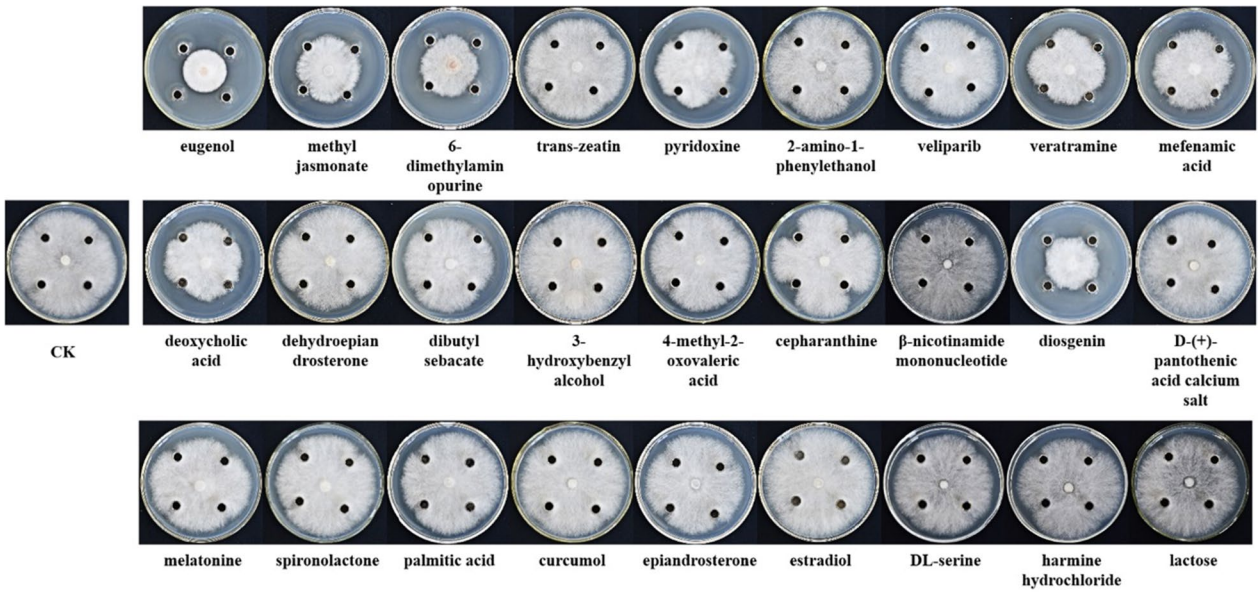

Fig. 4 Inhibition effect of different metabolites on Pn006

Table 7 Indoor toxicity measurements of three differential metabolites against Pn006

Differential metabolites	Virulence regression equation	EC_{50} (μg/mL)	R^2
Eugenol	$y = 0.1404X + 3.6241$	27.87	0.9689
Methyl jasmonate	$y = 0.1158X + 3.7972$	69.18	0.9564
6-Dimethylaminopurine	$y = 0.1402X + 2.4986$	55.09	0.986

effects (Fig. 4). The three chemicals mentioned above were, therefore, chosen for additional validation.

Indoor toxicity determination. The regression equation of the toxicity of each metabolite on Pn006 was calculated based on the results of the indoor toxicity assay (Table 7). Eugenol, methyl jasmonate, and 6-dimethylaminopurine all demonstrated strong inhibitory effects on Pn006, with eugenol exhibiting the best inhibitory effect with an EC_{50} value of 27.87 μg/mL.

Discussion

Pesticides can leave considerable residues in agricultural soils and crops when they are used extensively. The half-life of tebuconazole in the soil varies from a few weeks to a year and mainly depends on the quality of the soil and the initial residual concentration of tebuconazole [45]. Tebuconazole also harms soil ecology, suppresses soil fungi, and modifies soil microbial diversity [46]. Tebuconazole degraded slowly during the four repeated treatments, with the half-life initially increased and then decreased, according to research on the impact of tebuconazole on the soil by Han et al. [47]. Additionally, the variety of the soil microbial biomass and bacterial community diversity were both significantly decreased. Tebuconazole stimulated the proliferation of organotrophic bacteria and inhibited that of actinobacteria. It was to be a strong inhibitor of urease and catalase activities, while in turn, it enhanced the activities of dehydrogenases, acid phosphatase, alkaline phosphatase, and arylsulfatase [48]. However, there have also been reports that tebuconazole when administered at prescribed doses did not significantly disturb the biological homeostasis of soil and did not diminish its fertility. It also stimulates the proliferation of organotrophic bacteria and fungi, and also the activities of soil enzymes responsible for phosphorus, sulfur, and carbon metabolism [49]. Therefore, the effect of tebuconazole on soil is related to the dose at which it is applied. Fungi were found to be more responsive to the fungicide propiconazole than bacteria when its impact on soil microorganisms was examined. And while it does not affect basal respiration, it dramatically inhibits substrate-induced respiration [50]. The urease and phosphatase activities at lower propiconazole concentrations up. The microbial growth and urease and phosphatase activities were relentlessly reduced at higher propiconazole concentrations [51]. Therefore,

similar to tebuconazole, the effects of propiconazole on soil enzyme activity and microorganisms are related to its concentration.

Bacillus can promote plant growth and improve soil activity. Grapes treated with *Bacillus velezensis* strain GUMT319 displayed a notable increase in production and a higher concentration of soil microorganisms [52]. Application of microbial inoculants (containing effective strains of *Bacillus megaterium* and *Bacillus mucilaginous*) significantly increased chili pepper yield, inter-root soil fast-acting phosphorus and fast-acting potassium content. It did not significantly affect the diversity and composition of the soil bacterial community but increased the relative abundance of the bacterial genus Flavobacterium, responsible for promoting root development throughout the growth phase [53]. In organic maize pots, inoculants resulted in higher biomasses of bacteria, fungi, and actinomycetes compared to the control. Microbial inoculation may cause tremendous changes in the number and composition of the taxonomic groups [54]. These changes may influence plants and soil and thereby induce unpredictable feedback reactions [55]. Through qualitative or quantitative analysis of the levels of endogenous metabolites in organisms in a certain period, metabolomics has a certain guiding significance in exploring the relationship between metabolites and physiopathological changes, as well as the mechanism of drug therapy [56]. Endogenous cellular metabolites can be precisely detected and identified, revealing their metabolic routes and processes. This information can lead to new insights into the development, prevention, and treatment of diseases. Nuclear magnetic resonance (NMR), gas-mass spectrometry (GC–MS), liquid-mass spectrometry (LC–MS), and capillary electrophoresis (CE) are currently used assays in metabolomics. Among these, metabolomics by LC–MS is widely used due to its straightforward sample pre-treatment and comprehensive metabolite database information [57].

Cellular metabolomics studies are used to explain the mechanism of action by comparing the differences in concentrations of each metabolite between multiple groups and identifying key metabolites associated with the development and treatment of diseases or disorders. The experimental results showed that all nine combinations of the extracellular metabolites of Czk1 and the chemical fungicide Genkang were effective against the brown root rot disease fungus of the rubber tree (Pn006), with a volume ratio of Czk1 and Genkang of 2:8 having the highest efficacy. The method of action of the complex was discovered to be different from that of the single doses of the biocontrol fungus Czk1 and Genkang when Pn006 was studied by LC–MS/MS for differential changes in metabolites under stress by a strong synergistic mycorrhizal drug combination. The complexes changed the levels of several metabolites in the cells of Pn006. A total of 105 important differential metabolites were screened, and the complexes had new inhibitory effects. Disorders of lipid peroxidation, energy metabolism, auxin biosynthesis, and nucleotide metabolism in cells may be linked to these important metabolites.

Coenzyme A is a cofactor in intracellular metabolism and is widely distributed in all areas of life, including eukaryotes, bacteria and archaea [58]. It is involved in sugar, lipid, protein and energy metabolism and is produced through pyruvate oxidation and secondary metabolites of the tricarboxylic acid cycle [59]. Pantothenic acid is an important precursor for the synthesis of coenzyme A [60], which can be synthesized by enzymatic reactions in both plants and microorganisms [15, 61]. Pathogenic fungi of pantothenic acid content considerably increased following treatment with a compounding agent, indicating that these agents stimulate pantothenic acid production, which in turn controls the synthesis of coenzyme A and, in turn, indirectly affects cellular lipid and energy metabolism. Additionally, the buildup of nicotinamide mononucleotide (NMN), a significant synthetic precursor of intracellular coenzyme I (NAD+), which is essential for cellular antioxidation, energy metabolism, and genomic stability, was also noted [62]. The level of NMN was significantly increased in the CK-CG group compared to the control, rising 3.35 times, and NMN conversion was inhibited. The mechanism for the manufacture of NAD+ may have been hampered, which would have had an impact on the rate of lipid peroxidation and cell energy metabolism.

The polyunsaturated fatty acid alpha-linolenic acid is extremely sensitive to oxidative processes and strongly correlates with lipid peroxidation in cells [63]. In this study, there was a 7.81-fold increase in the content of alpha-linolenic acid in the compound that appeared to be very significantly upregulated, indicating that the metabolic activity of alpha-linolenic acid was significantly inhibited and that alpha-linolenic acid could not be properly metabolized into docosahexaenoic acid (DHA) and eicosapentaenoic acid (EPA), causing problems with cellular lipid metabolism. To some extent, the increased linolenic acid concentration raises the level of lipid peroxidation in cells. It has been demonstrated that too much linolenic acid makes cells more susceptible to lipid peroxidation [64]. Furthermore, it was discovered that the jasmonic acid content of pathogenic fungi decreased after treatment with compounding agents, possibly due to the down-regulation of the linolenic acid metabolic pathway. This result implies that the synthesis mechanism of jasmonic acid in fungi is comparable to the

synthesis pathway in plants, which utilizes linolenic acid as a synthetic substrate, as also documented in the investigations of Dong and Sun [65, 66].

Leucine and isoleucine levels were 3.32 and 5.54 times greater than the control in this study, indicating that the degradation mechanisms for valine, leucine, and isoleucine were dramatically downregulated. Leucine and isoleucine are branched-chain amino acids that serve as precursors to acetyl coenzyme A, an essential component of energy metabolism. By inhibiting either amino acid of degradation pathway, acetyl coenzyme A levels were significantly reduced, which interfered with the TCA cycle and the production of cellular energy [67, 68]. Pyruvate is produced in the cytoplasm by the glycolytic pathway and is present in eukaryotic cells and many prokaryotic cells [69] and is an important metabolite in the tricarboxylic acid cycle, participating in aerobic and anaerobic respiration of cells and is essential for maintaining normal cellular energy metabolism [70]. In this study, we found a 2.47-fold increase in pyruvate content in pathogenic bacteria (Pn006) cells treated with the compounding agent, but no change in lactate content was found, indicating no significant change in anaerobic respiration in which pyruvate is involved. The compounded drug reduced succinate in the group it was administered to by a factor of 0.39, indicating that the pathogen cells of the TCA cycle was disrupted, impairing pyruvate catabolism and leading to a large buildup of pyruvate. Succinate is a crucial substrate for the TCA cycle. This supports the conclusions reached by Chen et al. [71]. The accumulation of pyruvate was associated with a large consumption of sugars in pathogenic fungi. Trehalose, lactose, honey disaccharide, cottonseed sugar, and sucrose showed varying degrees of down-regulation, reflecting that pathogenic fungi undergo a large amount of energy metabolism to maintain normal cellular life activities after stress by compounding agents, which is similar to the findings of Lv et al. [72].

Additionally, because of the slow TCA cycle, pyruvate is not properly oxidized and broken down, which encourages the content of pyruvate to rise. Eugenol, methyl jasmonate, and 6-dimethylaminopurine were also discovered to have substantial inhibitory efficacy against pathogenic fungi when the inhibitory effect of 27 important differently metabolized chemicals was tested. Eugenol is a phenolic molecule of the phenylpropanoid group that exhibits antioxidant, fungicidal, and antiviral effects. It also affects cellular respiration and photosynthesis by compromising the integrity and permeability of cell membranes [73–75]. By interfering with the function of related enzymes and altering synthetic pathways, it can also prevent the growth of fungi [76]. Eugenol treatment caused the cytoplasmic walls of rice *Rhizoctonia solani* to separate, vesicles and mitochondria to shrink or dissolve, the synthesis of ergosterol to be blocked, and changes to the amino acid and glucose transport across the cell membrane [77]. Methyl jasmonate is a linoleic acid-derived cyclopentanone compound, and treatment of *B. dothidea* with methyl jasmonate inhibits its respiratory metabolism through the tricarboxylic acid cycle and suppresses ATP, DNA, and protein synthesis [78]. 6-Dimethylaminopurine is a serine/threonine kinase inhibitor, and Bhandari found that the metabolite of Streptomyces 6-dimethylaminopurine was found to have a good inhibitory effect after molecular docking [79]. Fungi can produce a wide range of metabolites, including hazardous natural compounds [80]. The study of metabolomes still faces many obstacles and limitations, and the existence of metabolites generated from fungi makes it more difficult to conduct metabolomic research on plant-pathogen interactions. This makes the interpretation of the obtained metabolites more difficult, and the establishment of a comprehensive metabolite database of pathogenic fungi is expected to help overcome this obstacle [81].

In summary, this study demonstrated that the combination of Czk1 and Genkang significantly inhibited the cell viability of Pn006 from a metabolomic perspective, and together they exerted a synergistic effect. The mechanism of action may involve interfering with the manufacture of coenzymes and energy metabolism in pathogenic fungi cells to inhibit and potentiate the growth of the fungi. In this study, only a preliminary investigation of the mechanism of inhibition and synergism of Czk1 in combination with the chemical fungicide (Genkang) was carried out. To fully reflect the synergistic mechanism of the Czk1 in combination with Genkang, multi-omics analysis and further validation with genome, transcriptome, and proteome are required in the future.

Conclusion

The chemical fungicide Genkang, in combination with Czk1, significantly inhibited and strong synergistic on Pn006, with the strongest synergistic effect when the combined volume ratio Czk1: Genkang = 2:8 and the increase ratio was 1.49. The LC–MS/MSbased non-target metabolomics research revealed that the fungicide-bacterial combination of 105 important metabolites was screened from a total of 708 distinct differential metabolites. The metabolism of linolenic acid and the degradation of valine, leucine, and isoleucine were the unique differential metabolic pathways of the combination. Specific synergies mechanisms are as follows. The increase in the content of α-linolenic acid in Pn006 cells increased the sensitivity of Pn006 to oxidative reactions and the degree of cellular lipid peroxidation increased.

The activities of antioxidant enzymes POD and SOD in Pn006 cells were reduced, which severely weakened the ability of Pn006 to cope with oxidative stress, and further led to the gradual accumulation of free radicals in Pn006 cells, thus accelerating cellular senescence and death. By interfering with the content of succinic acid, it slows down the process of Pn006 energy, thus reducing the ability of Pn006 to cope with various stresses. Destroying the cell membrane structure, prompting the leakage of cell contents, leading to the disruption of the ion and water balance inside and outside the cell, further destroying the balance of protoplasts, and interfering with the normal physiological functions of the cell. Chemical fungicides enhance the ability of cellulase secretion by biocontrol bacteria so that biocontrol bacteria can destroy the cell wall of Pn006 more effectively and weaken the competitive ability of Pn006, which is conducive to the colonization of biocontrol bacteria as well as exerting the other bacterial inhibitory ability of biocontrol bacteria.

Abbreviations

Genkang	25% Propiconazole–tebuconazole
LC–MS/MS	Liquid chromatography–tandem mass spectrometry
Czk1	*Bacillus subtilis* Czk1
Pn006	*Pyrrhoderma noxium* Pn006
IR	Increase ratio
PCA	Principal component analysis
ESI+	Positive electron spray ionization
ESI−	Negative electron spray ionization
CK-CG	Compound groups
CK-C	*Bacillus subtilis* Czk1 groups
CK-G	Genkang groups
VIP	Importance in Projection
FC	Fold Change
LC–MS	Liquid Chromatograph with Mass Spectrometry
NMN	Nicotinamide mononucleotide
NAD+	Coenzyme I

Supplementary Information

The online version contains supplementary material available at https://doi.org/10.1186/s40538-023-00487-4.

Additional file 1: Fig. S1. Grouped PCA analysis model. a-c: PCA model in positive ion mode; d-f: PCA model in negative ion mode.

Additional file 2: Table S1. Changes in key metabolites in the CK-CG group (positive ion mode).

Acknowledgements
Not applicable.

Author contributions
ZG, JY and HW experimented and did data analysis. YL, YL, WW, RL, ST, CH and KY supervised the project. JY, YL and CH designed the study. ZG, JY, HW and CH participated in writing the manuscript. All authors read and approved the final manuscript.

Funding
Supported by Hainan Provincial Natural Science Foundation of China, (Grant No. 320RC692, No. 322QN360); The specific research fund of The Innovation Platform for Academicians of Hainan Province (Grant No. SQ2020PTZ0011); The Earmarked Fund for China Agriculture Research System (Grant No. CARS-33-BC1).

Availability of data and materials
The data used in this study are completely provided during submission.

Declarations

Ethics approval and consent to participate
Not applicable.

Consent for publication
Not applicable.

Competing interests
The authors declare that they have no competing interests.

Author details
[1]School of Tropical Agriculture and Forestry, Hainan University, Haikou 570228, China. [2]Environment and Plant Protection Institute, Chinese Academy of Tropical Agricultural Science, Key Laboratory of Integrated Pest Management on Tropical Crops, Ministry of Agriculture and Rural Affairs, Haikou 571101, People's Republic of China. [3]College of Agriculture, Guizhou University, Guiyang 550025, China. [4]College of Agronomy and Biotechnology, Yunnan Agricultural University, Kunming 650201, China. [5]Sanya Research Institute of Chinese Academy of Tropical Agricultural Sciences, Sanya 572025, China. [6]Hainan Key Laboratory for Monitoring and Control of Tropical Agricultural Pests, Haikou 571101, China. [7]Hainan Engineering Research Center for Biological Control of Tropical Crops Diseases and Insect Pests, Haikou 571101, China.

Received: 18 July 2023 Accepted: 3 October 2023
Published online: 16 October 2023

References

1. Longsaward R, Pengnoo A, Kongsawadworakul P, Viboonjun U. A novel rubber tree PR-10 protein involved in host-defense response against the white root rot fungus *Rigidoporus microporus*. BMC Plant Biol. 2023;23(1):157. https://doi.org/10.1186/s12870-023-04149-3.
2. Ann PJ, Chang TT, Ko WH. *Phellinus noxius* brown root rot of fruit and ornamental trees in Taiwan. Plant Dis. 2002;86(8):820–6. https://doi.org/10.1094/PDIS.2002.86.8.820.
3. Du P, Wu C, Zhou L, Wu F, Dai Y. Notes on the nomenclature of three entry tree quarantine fungi. Mycosystema. 2020;39(8):1603–6. https://doi.org/10.13346/j.mycosystema.200022.
4. Liu YX, Shi YP, Dai LM, Li LL, Cai ZY. Screening, identification and fermentation optimization of an antimicrobial actinomycete strain 17–7 to *Phellinus noxius*. Microbiol China. 2020;47(01):118–29. https://doi.org/10.13344/j.microbiol.china.190160.
5. Liang Y, Li R, Wu W, Xi J, Tan S, Huang X, Lu Y, He C, Yi K. Inhibitory mechanism of volatilized active components from *Bacillus subtilis* Czk1 on *Ganoderma pseudoferreum*. J Agric Sci Technol. 2022;24(2):152–9. https://doi.org/10.13304/j.nykjdb.2020.0991.
6. Ann PJ, Lee HL, Huang TC. Brown root rot of 10 species of fruit trees caused by *Phellinus noxius* in Taiwan. Plant Dis. 1999;83(8):746–50. https://doi.org/10.1094/PDIS.1999.83.8.746.
7. He C, Li R, Wu W, Zheng X, Wu C, Liang Y. Evaluation of 12 fungicides for Suppression of *Phellinus noxius*. Chin J Ecol. 2013;34(10):1987–90. https://doi.org/10.3969/j.issn.1000-2561.2013.10.023.
8. Wang Y, Meng H, Gu V, Gu J. Molecular diagnosis of the brown root rot disease agent *Phellinus noxius* on trees and in soil by rDNA ITS analysis. Appl Environ Microbiol. 2016;1(1):81–91. https://doi.org/10.26789/AEB.2016.01.002.
9. Palasak J, Buppasang R, Kachangoon R, et al. Preconcentration of triazole fungicides using effervescent assisted switchable hydrophilicity solvent-based microextraction prior to high-performance liquid chromatographic analysis. Microchem J. 2022;182: 107882. https://doi.org/10.1016/j.microc.2022.107882.

10. Xu Y, Zhang Y, Tao Q, et al. A possible but unrecognized risk of acceptable daily intake dose triazole pesticides exposure-bile acid disturbance induced pharmacokinetic changes of oral medication. Chemosphere. 2023;322: 138209. https://doi.org/10.1016/j.chemosphere.2023.138209.
11. Wang Q, Long Y, Ai Q, Su Y, Lei Y. Oligosaccharins used together with tebuconazole enhances resistance of kiwifruit against soft rot disease and improves its yield and quality. Horticulturae. 2022;8(7):624. https://doi.org/10.3390/horticulturae8070624.
12. Seham MH, Inas JAL, Shereen MK, Emad AA, Hussein SM, Hamada A. Hazard assessment and environmental fate of propiconazole degradation by microalgae: differential tolerance, antioxidant and detoxification pathway. J Environ Chem Eng. 2022;10(4): 108170. https://doi.org/10.1016/j.jece.2022.108170.
13. Lucas JA, Hawkins NJ, Fraaije BA. The evolution of fungicide resistance. Adv Appl Microbiol. 2015;90(29):29–92. https://doi.org/10.1016/bs.aambs.2014.09.001.
14. Elad Y, Zimand GY, Zaqs Y, Zuriel S, Chet I. Use of *Trichoderma harzianum* in combination or alternation with fungicides to control cucumber grey mould (*Botrytis cinerea*) under commercial greenhouse conditions. Plant Pathol. 1993;42(3):324–32. https://doi.org/10.1111/j.1365-3059.1993.tb01508.x.
15. Kashyap AS, Manzar N, Nebapure SM, et al. Unraveling microbial volatile elicitors using a transparent methodology for induction of systemic resistance and regulation of antioxidant genes at expression levels in chili against bacterial wilt disease. Antioxidants (Basel). 2022;11(2):404. https://doi.org/10.3390/antiox11020404.
16. Barakat RM, Al-Masri MI. Effect of *Trichoderma harzianum* in combination with fungicides in controlling gray mould disease (*Botrytis cinerea*) of strawberry. AM J Plant Sci. 2017;8(4):651. https://doi.org/10.4236/ajps.2017.84045.
17. Chen Z, Ren H, Liu Y, Xu Z. Synergism between tebuconazole and *Bacillus subtilis* against faba bean fusarium wilt and mechanism of increasing effect. Chin J Pesticide Sci. 2002;4(4):40–4. https://doi.org/10.3321/j.issn:1008-7303.2002.04.008.
18. Wang YF. Control Efficiency and Mechanism of Biocontrol Bacteria and Pesticides on Bitter gourd *Fusarium* Wilt. Shandong Agric Univ. 2019.
19. Shang D, Liu Y, Jiang F, Ji F, Wang H, Han X. Synergistic antibacterial activity of designed Trp-containing antibacterial peptides in combination with antibiotics against multidrug-resistant *Staphylococcus epidermidis*. Front Microbiol. 2019;10:2719. https://doi.org/10.3389/fmicb.2019.02719.
20. Narware J, Singh SP, Manzar N, Kashyap AS. Biogenic synthesis, characterization, and evaluation of synthesized nanoparticles against the pathogenic fungus *Alternaria solani*. Front Microbiol. 2023;14:1159251. https://doi.org/10.3389/fmicb.2023.1159251.
21. Daranas N, Roselló G, Cabrefiga J, et al. Biological control of bacterial plant diseases with *Lactobacillus plantarum* strains selected for their broad-spectrum activity. Ann Appl Biol. 2019;174(1):92–105. https://doi.org/10.1111/aab.12476.
22. Kashyap AS, Manzar N, Meshram S, Sharma PK. Screening microbial inoculants and their interventions for cross-kingdom management of wilt disease of solanaceous crops- a step toward sustainable agriculture. Front Microbiol. 2023;14:1174532. https://doi.org/10.3389/fmicb.2023.1174532.
23. Yadav DK, Devappa V, Kashyap AS, et al. Boosting the biocontrol efficacy of *Bacillus amyloliquefaciens* DSBA-11 through physical and chemical mutagens to control bacterial wilt disease of tomato caused by *Ralstonia solanacearum*. Microorganisms. 2023;11(7):1790. https://doi.org/10.3390/microorganisms11071790.
24. Kashyap AS, Manzar N, Rajawat MVS, et al. Screening and biocontrol potential of rhizobacteria native to gangetic plains and hilly regions to induce systemic resistance and promote plant growth in chilli against bacterial wilt disease. Plants (Basel). 2021;10(10):2125. https://doi.org/10.3390/plants10102125.
25. Malik MS, Rehman A, Khan IU, et al. Thermo-neutrophilic cellulases and chitinases characterized from a novel putative antifungal biocontrol agent: *Bacillus subtilis* TD11. PLoS ONE. 2023;18(1): e0281102. https://doi.org/10.1371/journal.pone.0281102.
26. Kumbar B, Mahmood R, Nagesha SN, et al. Field application of *Bacillus subtilis* isolates for controlling late blight disease of potato caused by *Phytophthora infestans*. Biocatal Agric Biotechnol. 2019;22: 101366. https://doi.org/10.1016/j.bcab.2019.101366.
27. Yi Y, Li Z, Song C, Kuipers OP. Exploring plant-microbe interactions of the rhizobacteria *Bacillus subtilis* and *Bacillus mycoides* by use of the CRISPR-Cas9 system. Environ Microbiol. 2018;20(12):4245–60. https://doi.org/10.1111/1462-2920.14305.
28. Ons L, Bylemans D, Thevissen K, Cammue BPA. Combining biocontrol agents with chemical fungicides for integrated plant fungal disease control. Microorganisms. 2020;8(12):1930. https://doi.org/10.3390/microorganisms8121930.
29. Derbalah AS, El Kot GA, Hamza AM. Control of powdery mildew in okra using cultural filtrates of certain bio-agents alone and mixed with penconazole. Arch Phytopathol Pflanzenschutz. 2011;44(20):2012–23. https://doi.org/10.1080/03235408.2011.559041.
30. Li XJ, Yao CX, Qiu R, et al. Isolation, identification, and evaluation of the biocontrol potential of a *Bacillus velezensis* strain against tobacco root rot caused by *Fusarium oxysporum*. J Appl Microbiol. 2023;134(1): lxac049. https://doi.org/10.1093/jambio/lxac049.
31. Omar I, O'Neill TM, Rossall S. Biological control of fusarium crown and root rot of tomato with antagonistic bacteria and integrated control when combined with the fungicide carbendazim. Plant Pathol. 2010;55(1):92–9. https://doi.org/10.1111/j.1365-3059.2005.01315.x.
32. Qin Y, Tu M, Yang M, Qi J, Tang C. Antagonistic effect of eight strains of *Trichoderma* on *Ganoderma pseudoferreum* causing red root rot of rubber tree. Chin J Trop Agric. 2015;35(3):41–5. https://doi.org/10.3969/j.issn.1009-2196.2015.03.010.
33. Nakaew N, Rangjaroen C, Sungthong R. Utilization of rhizospheric Streptomyces for biological control of *Rigidoporus* sp. causing white root disease in rubber tree. Eur J Plant Pathol. 2015;142(1):93–105. https://doi.org/10.1007/s10658-015-0592-0.
34. Liang Y, Li R, Wu W, et al. Inhibition of volatile organic compounds produced by *Bacillus subtilis* Czk1 on red root of rubber tree. J Agric Sci Technol. 2020;22(11):116–23. https://doi.org/10.13304/j.nykjdb.2020.0378.
35. Li H, Tang C, Yang M, Qi J, Qin Y. Antagonistic effects of *Trichoderma* strains on *Phellinus noxius* in *Hevea brasilliensis*. Fujian Agric Sci. 2015;30(4):362–6. https://doi.org/10.3969/j.issn.1008-0384.2015.04.010.
36. Zahari R, Halimoon N, Ahmad MF, Ling SK. Antifungal compound isolated from *Catharanthus roseus* L. (Pink) for biological control of root rot rubber diseases. Int J Anal Chem. 2018;2018:8150610. https://doi.org/10.1155/2018/8150610.
37. He CP, Fan LY, Wu WH, et al. Identification of lipopeptides produced by *Bacillus subtilis* Czk1 isolated from the aerial roots of rubber trees. Genet Mol Res. 2017;16(1):1–13. https://doi.org/10.4238/gmr16018710.
38. Roessner U, Bowne J. What is metabolomics all about? Biotechniques. 2009;46(5):363. https://doi.org/10.2144/000113133.
39. Isha A, Yusof NA, Shaari K, Osman R, Wong MY. Metabolites identification of oil palm roots infected with *Ganoderma boninense* using GC-MS-based metabolomics. Arab J Chem. 2020;13(7):6191. https://doi.org/10.1016/j.arabjc.2020.05.026.
40. Zhu L, Zhou Y, Li X, Zhao J, Guo N, Xing H. Metabolomics analysis of soybean hypocotyls in response to *Phytophthora sojae* infection. Front Plant Sci. 2018;9:1530. https://doi.org/10.3389/fpls.2018.01530.
41. Fernando K, Reddy P, Guthridge KM, Spangenberg GC, Rochfort SJ. A metabolomic study of *Epichloë* endophytes for screening antifungal metabolites. Metabolites. 2022;12(1):37. https://doi.org/10.3390/metabo12010037.
42. Kumaraswamy GK, Bollina V, Kushalappa AC, et al. Metabolomics technology to phenotype resistance in barley against *Gibberella zeae*. Eur J Plant Pathol. 2011;130(1):29–43. https://doi.org/10.1007/s10658-010-9729-3.
43. Xie L. Synergistic control of rubber root disease and anthracnose by *Bacillus subtilis* Czk1 and chemical fungicide. Hainan Univ. 2020.
44. Horsfall JG, Barratt RW. An improved grading system for measuring plant disease. Phytopathology. 1945;35:45–9.
45. Cui N, Xu H, Yao S, He Y, Zhang H, Yu Y. Chiral triazole fungicide tebuconazole: enantioselective bioaccumulation, bioactivity, acute toxicity, and dissipation in soils. Environ Sci Pollut Res Int. 2018;25(25):25468–75. https://doi.org/10.1007/s11356-018-2587-9.
46. Muñoz-Leoz B, Ruiz-Romera E, Antigüedad I, Garbisu C. Tebuconazole application decreases soil microbial biomass and activity. Soil Biol Biochem. 2011;43(10):2176–83. https://doi.org/10.1016/j.soilbio.2011.07.001.
47. Han L, Kong X, Xu M, Nie J. Repeated exposure to fungicide tebuconazole alters the degradation characteristics, soil microbial community and

functional profiles. Environ Pollut. 2021;287: 117660. https://doi.org/10.1016/j.envpol.2021.117660.
48. Bamaga M, Wyszkowska J, Kucharski J. Bacterial diversity and enzymatic activity in a soil recently treated with tebuconazole. Ecol Indic. 2021;123(2): 107373. https://doi.org/10.1016/j.ecolind.2021.107373.
49. Baćmaga M, Wyszkowska J, Borowik A, Kucharski J. Effects of tebuconazole application on soil microbiota and enzymes. Molecules. 2022;27(21):7501. https://doi.org/10.3390/molecules27217501.
50. Fernández-Calviño D, Rousk J, Bååth E, Bollmann UE, Bester K, Brandt KK. Ecotoxicological assessment of propiconazole using soil bacterial and fungal growth assays. Appl Soil Ecol. 2017;115:27–30. https://doi.org/10.1016/j.apsoil.2017.03.009.
51. Satapute P, Kamble MV, Adhikari SS, Jogaiah S. Influence of triazole pesticides on tillage soil microbial populations and metabolic changes. Sci Total Environ. 2019;651(Pt 2):2334–44. https://doi.org/10.1016/j.scitotenv.2018.10.099.
52. Chen X, Yang F, Bai C, et al. *Bacillus velezensis* strain GUMT319 reshapes soil microbiome biodiversity and increases grape yields. Biology (Basel). 2022;11(10):1486. https://doi.org/10.3390/biology11101486.
53. Zhao Y, Zhang M, Yang W, et al. Effects of microbial inoculants on phosphorus and potassium availability, bacterial community composition, and chili pepper growth in a calcareous soil: a greenhouse study. J Soils Sediments. 2019. https://doi.org/10.1007/s11368-019-02319-1.
54. Angelina E, Papatheodorou EM, Demirtzoglou T, Monokrousos N. Effects of *Bacillus subtilis* and *Pseudomonas fluorescens* inoculation on attributes of the lettuce (*Lactuca sativa* L.) soil rhizosphere microbial community: the role of the management system. Agronomy. 2020;10:1428. https://doi.org/10.3390/agronomy10091428.
55. Trabelsi D, Mhamdi R. Microbial inoculants and their impact on soil microbial communities: a review. Biomed Res Int. 2013;2013: 863240. https://doi.org/10.1155/2013/863240.
56. Katam R, Lin C, Grant K, Katam CS, Chen S. Advances in plant metabolomics and its applications in stress and single-cell biology. Int J Mol Sci. 2022;23(13):6985. https://doi.org/10.3390/ijms23136985.
57. Arbona V, Iglesias DJ, Talón M, Gómez-Cadenas A. Plant phenotype demarcation using nontargeted LC-MS and GC-MS metabolite profiling. J Agric Food Chem. 2009;57(16):7338–47. https://doi.org/10.1021/jf9009137.
58. Leonardi R, Zhang YM, Rock CO, Jackowski S. Coenzyme A: back in action. Prog Lipid Res. 2005;44(2–3):125–53. https://doi.org/10.1016/j.plipres.2005.04.001.
59. Suryatin AG, Iwatani T, Okano K, Kitani S, Honda K. In vitro production of coenzyme a using thermophilic enzymes. Appl Environ Microbiol. 2021;87(14): e0054121. https://doi.org/10.1128/AEM.00541-21.
60. Pourcel L, Buron F, Garcia F, et al. Transient vitamin B_5 starving improves mammalian cell homeostasis and protein production. Metab Eng. 2020;60:77–86. https://doi.org/10.1016/j.ymben.2020.03.008.
61. Chakauya E, Coxon KM, Whitney HM, Ashurst JL, Abell C, Smith AG. Pantothenate biosynthesis in higher plants: advances and challenges. Physiol Plant. 2006;126(3):319–29. https://doi.org/10.1111/j.1399-3054.2006.00683.x.
62. Odoh CK, Guo X, Arnone JT, Wang X, Zhao ZK. The role of NAD and NAD precursors on longevity and lifespan modulation in the budding yeast, *Saccharomyces cerevisiae*. Biogerontology. 2022;23(2):169–99. https://doi.org/10.1007/s10522-022-09958-x.
63. Yadav RK, Singh M, Roy S, Ansari MN, Saeedan AS, Kaithwas G. Modulation of oxidative stress response by flaxseed oi: Role of lipid peroxidation and underlying mechanisms. Prostaglandins Other Lipid Mediat. 2018;135:21–6. https://doi.org/10.1016/j.prostaglandins.2018.02.003.
64. Couëdelo L, Buaud B, Abrou H, Chamekh-Coelho I, Majou D, Boué-Vaysse C. Effect of increased levels of dietary α-linolenic acid on the n-3 PUFA bioavailability and oxidative stress in rat. Br J Nutr. 2022;127(9):1320–33. https://doi.org/10.1017/S0007114521002294.
65. Dong WH. Study on fermentative production of jasmonic acid by *Lasiodiplodia iranensis*. Jiangnan Univ. 2018.
66. Sun XY. Study on the synthesis pathway of jasmonic acid produced by *Lasiodiplodia iranensis*. Jiangnan Univ. 2020.
67. Ahuja R, Agrawal N, Kumar H, Kumar V. Emerging role of branched chain amino acids in metabolic disorders A mechanistic review. Pharmanutrition. 2018;6(2):47–54. https://doi.org/10.1016/j.phanu.2018.01.003.
68. Shimomura Y, Kitaura Y. Physiological and pathological roles of branched-chain amino acids in the regulation of protein and energy metabolism and neurological functions. Pharmacol Res. 2018;133:215–7. https://doi.org/10.1016/j.phrs.2018.05.014.
69. Cybulski K, Tomaszewska-Hetman L, Rakicka M, Juszczyk P, Rywińska A. Production of pyruvic acid from glycerol by *Yarrowia lipolytica*. Folia Microbiol (Praha). 2019;64(6):809–20. https://doi.org/10.1007/s12223-019-00695-2.
70. Zhang HY, Tan XX, Kang K, Wang W, Lian KQ, Kang WJ. Simultaneous determination of lactic acid and pyruvic acid in tissue and cell culture media by gas chromatography after in situ derivatization-ultrasound-assisted emulsification microextraction. Anal Bioanal Chem. 2019;411(3):787–95. https://doi.org/10.1007/s00216-018-1502-z.
71. Chen C, Cai N, Chen J, Wan C. UHPLC-Q-TOF/MS-based metabolomics approach reveals the antifungal potential of pinocembroside against *Citrus* green mold phytopathogen. Plants (Basel). 2019;9(1):17. https://doi.org/10.3390/plants9010017.
72. Lv N, Ma K, Li R, Liang P, Liang P, Gao X. Sublethal and lethal effects of the imidacloprid on the metabolic characteristics based on high-throughput non-targeted metabolomics in *Aphis gossypii* Glover. Ecotoxicol Environ Saf. 2021;212: 111969. https://doi.org/10.1016/j.ecoenv.2021.111969.
73. Philippe S, Farougou S, Ahounou S, et al. Comparative study of antifungal activities of six selected essential oils against fungal isolates from cheese wagashi in Benin. Pak J Biol Sci. 2013;16(23):1751–7. https://doi.org/10.3923/pjbs.2013.1751.1757.
74. Tworkoski T. Herbicide effects of essential oils. Weed Sci. 2002;50:425–31. https://doi.org/10.1614/0043-1745(2002)050[0425:HEOEO]2.0.CO;2.
75. Anjali, Sumit K, Tulasi K, et al. Role of plant secondary metabolites in defence and transcriptional regulation in response to biotic stress. Plant Stress. 2023;8: 100154. https://doi.org/10.1016/j.stress.2023.100154.
76. Darvishi E, Omidi M, Bushehri AA, Golshani A, Smith ML. The antifungal eugenol perturbs dual aromatic and branched-chain amino acid permeases in the cytoplasmic membrane of yeast. PLoS ONE. 2013;8(10):1–9. https://doi.org/10.1371/journal.pone.0076028.
77. Zhao Y, Wang Q, Wu X, et al. Unraveling the polypharmacology of a natural antifungal product, eugenol, against *Rhizoctonia solani*. Pest Manag Sci. 2021;77(7):3469–83. https://doi.org/10.1002/ps.6400.
78. Li XQ. Effect of Methyl Jasmonate on Bacteriostatic Action and Metabolic Enzyme Activity of *Botryosphaeria dothidea*. Guizhou Univ. 2019.
79. Bhandari S, Bhattarai BR, Adhikari A, et al. Characterization of *Streptomyces* species and validation of antimicrobial activity of their metabolites through molecular docking. Processes. 2022;10(10):2149. https://doi.org/10.3390/pr10102149.
80. Wisecaver JH, Slot JC, Rokas A. The evolution of fungal metabolic pathways. PLoS Genet. 2014;10(12): e1004816. https://doi.org/10.1371/journal.pgen.1004816.
81. Aliferis KA, Jabaji S. Deciphering plant–pathogen interactions applying metabolomics: principles and applications. Can J Plant Pathol. 2012;34(1):29–33. https://doi.org/10.1080/07060661.2012.665388.

Publisher's Note